Analysis of Advanced Supercritical Carbon Dioxide Power Cycles With a Bottoming Cycle for Concentrating Solar Power Applications

Saeb M. Besarati
e-mail: sbesarati@mail.usf.edu

D. Yogi Goswami[1]
e-mail: goswami@usf.edu

Clean Energy Research Center,
University of South Florida,
4202 E. Fowler Avenue, ENB 118,
Tampa, FL 33620

A number of studies have been performed to assess the potential of using supercritical carbon dioxide (S-CO_2) in closed-loop Brayton cycles for power generation. Different configurations have been examined among which recompression and partial cooling configurations have been found very promising, especially for concentrating solar power (CSP) applications. It has been demonstrated that the S-CO_2 Brayton cycle using these configurations is capable of achieving more than 50% efficiency at operating conditions that could be achieved in central receiver tower type CSP systems. Although this efficiency is high, it might be further improved by considering an appropriate bottoming cycle utilizing waste heat from the top S-CO_2 Brayton cycle. The organic Rankine cycle (ORC) is one alternative proposed for this purpose; however, its performance is substantially affected by the selection of the working fluid. In this paper, a simple S-CO_2 Brayton cycle, a recompression S-CO_2 Brayton cycle, and a partial cooling S-CO_2 Brayton cycle are first simulated and compared with the available data in the literature. Then, an ORC is added to each configuration for utilizing the waste heat. Different working fluids are examined for the bottoming cycles and the operating conditions are optimized. The combined cycle efficiencies and turbine expansion ratios are compared to find the appropriate working fluids for each configuration. It is also shown that combined recompression-ORC cycle achieves higher efficiency compared with other configurations.
[DOI: 10.1115/1.4025700]

Introduction

Carbon dioxide is a nontoxic, abundant, inexpensive, nonflammable, and highly stable compound with low critical properties. It has been investigated as a working fluid for thermodynamic power cycles for many years.

Feher [1] designed the first supercritical CO_2 cycle in the United States in 1967. While the proposed cycle operates entirely above the critical pressure of CO_2, a pump is used for compression of the working fluid in the liquid phase. At the same time, Angelino [2] was working in Italy on designing a liquid phase compression gas turbine. He concluded that the efficiency of the resulting cycle is considerably higher than that of regenerative Brayton cycles and comparable with that of regenerative Rankine cycles. In 1968, he analyzed the thermodynamic performance of several carbon dioxide condensation cycles in which low temperature of the cycle is below critical temperature, and concluded that a recompression CO_2 cycle in which compression is performed while the working fluid is partially in liquid state achieves high efficiencies [3]. However, since the critical temperature of CO_2 is low (30.98 °C), it requires low temperature cooling water that is not available at many locations, especially at those with high solar resources. The low temperature cooling water limitation led to studies on the CO_2 cycle in gas state only. In 1969, Angelino [4] considered real gas effects and found higher cycle efficiency mainly due to the reduction of specific volume and compression work around critical point. Since then, S-CO_2 power cycles have drawn attention for nuclear power generation in gas reactors.

Dostal et al. [5] showed that the S-CO_2 cycle has a higher efficiency than the superheated steam cycle at temperatures above 470 °C, which makes it suitable for nuclear power applications. Sarkar [6,7] performed a detailed thermodynamic analysis and optimization of the cycle for a high temperature range of 480 °C–750 °C, considering a nuclear reactor as the heat source. Moisseytsev and Sienicki [8] investigated alternative layouts for S-CO_2 Brayton cycle for a sodium-cooled fast reactor (SFR), including double recompression, intercooling, and reheating. Jeong et al. [9] studied the potential improvement of the S-CO_2 cycle by mixing CO_2 with other gases in a SFR to alter its critical properties. The CO_2-He binary mixture showed the highest potential for efficiency improvement.

Although most of the studies so far have considered S-CO_2 for nuclear power applications, there is a growing interest in deploying it in CSP plants due to limitations of the current heat transfer fluids (HTF). Regular CSP plants use oil, molten salt, or steam as the HTF to absorb solar thermal energy in the receiver and transfer it to the working fluid in the power block. The maximum operating temperature of oil is 400 °C, which limits the performance of the power plant. Molten salt can be used at higher temperatures (around 560 °C), however, elaborate freeze protection systems are required. Direct steam generation requires complex control systems due to the phase change in the receiver, and the storage capacity is also limited [10]. On the other hand, CO_2 can be used at very high temperatures and is nontoxic, inexpensive, and nonflammable. Moreover, it can be directly used in a Brayton cycle to generate power, which eliminates the heat exchanger between the HTF and the working fluid. For these reasons, we have analyzed this cycle for concentrated solar power and have considered temperature conditions appropriate for CSP.

The performances of different S-CO_2 Brayton cycle configurations for central receiver solar power plants were theoretically

[1]Corresponding author.

Contributed by the Solar Energy Division of ASME for publication in the Journal of Solar Energy Engineering. Manuscript received June 17, 2013; final manuscript received August 30, 2013; published online November 19, 2013. Assoc. Editor: Aldo Steinfeld.

evaluated by Turchi et al. [11]. The results show that S-CO_2 Brayton cycle is able to achieve more that 50% efficiency under dry cooling conditions, which is consistent with the framework of the U.S. Department of Energy "SunShot Concentrating Solar Power R&D" program [12]. The main advantages of the S-CO_2 Brayton cycle can be summarized as high efficiency, high power density, compactness, and low cost [11].

Although the efficiency of the S-CO_2 Brayton cycle is high, it might be further improved by considering an appropriate bottoming cycle utilizing waste heat from the top S-CO_2 cycle. ORC is one of the alternatives, which is extensively used when the heat source temperature is below 370 °C [13]. However, the cycle performance is substantially affected by the selection of the working fluid. Chacartegui et al. [14] studied the performance of combined S-CO_2–ORC cycle with different working fluids under different operating conditions. The results showed that the efficiency of the S-CO_2 was improved by 7–12% points, depending on the turbine inlet temperature. It is noteworthy that the simple S-CO_2 configuration was considered for that study. In another study, Sánchez et al. [15] investigated the performance of a combined S-CO_2–ORC cycle using mixtures of hydrocarbons in the bottoming cycle. The results showed that the performance of the cycle is directly affected by the mixture's composition. It was concluded that doping the optimum pure fluid with a heavier fluid enhances the performance at higher temperatures, whereas doping with lighter fluid is more appropriate at lower temperatures. In that study also, the simple S-CO_2 configuration was considered as the top cycle.

In this paper, three different configurations of S-CO_2 Brayton cycle, i.e., simple, recompression, and partial cooling are considered as the top cycles providing heat for an organic Rankine bottoming cycle. The three configurations are first simulated and compared with the available data from the literature. Then, different working fluids are examined for the ORC for each configuration and the operating conditions are optimized. The combined cycle energy efficiencies and turbine expansion ratios are compared to find the appropriate working fluids for each configuration.

S-CO_2 Brayton Cycle Configurations

The three configurations considered in this study are called simple, recompression, and partial cooling cycles.

Simple Cycle. The simple cycle is the one from which the other two configurations are derived, which is shown in Fig. 1. High temperature S-CO_2 enters the turbine where it is expanded to the low pressure of the cycle. Next, it goes through the recuperator and transfers energy to the flow leaving the compressor. Then, it is cooled by rejecting heat to the cold sink and pressurized by the compressor, respectively. The pressurized S-CO_2 gains energy in the recuperator and exits to the heater. The cycle efficiency can be increased by dividing the compression into two stages and using an intercooler in between. Similarly, using a two stage expansion and a reheater can be beneficial.

Recompression Cycle. In recompression Brayton cycle, the flow is divided into two streams after leaving the low temperature recuperator (LTR). A fraction of the flow rejects heat to the cold sink and exits to the main compressor, while the other fraction is pressurized in a recompression compressor without cooling down (Fig. 2). The two streams are mixed at point 3, and the mixed stream enters a high temperature recuperator (HTR) and a heater, where thermal energy is added to achieve the required turbine inlet temperature. After expanding in the turbine, the flow is directed into HTR and LTR to preheat the high pressure stream.

The main advantage of the recompression cycle over the simple configuration is better heat recovery. Splitting the flow after the LTR decreases the heat capacity of the high pressure side in LTR

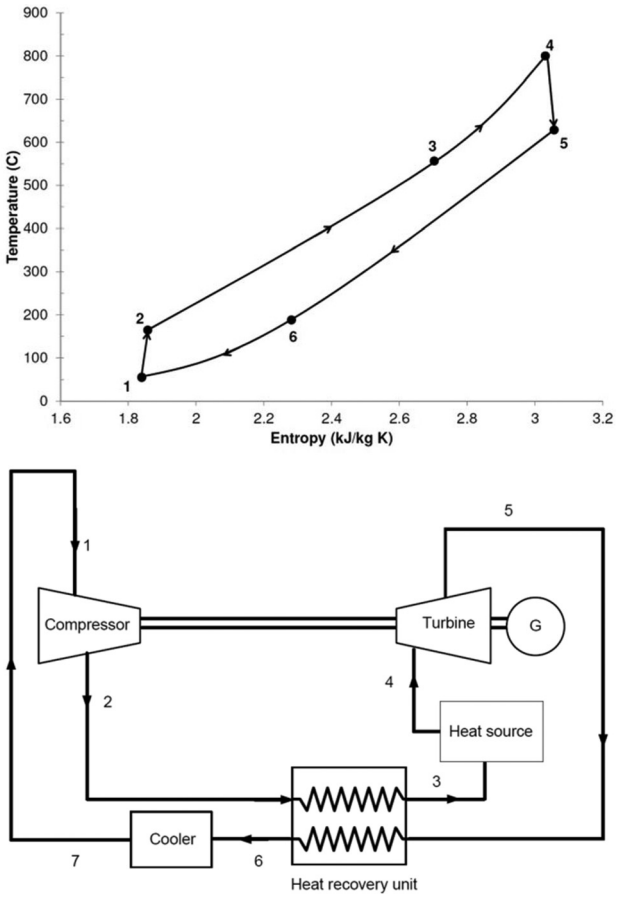

Fig. 1 Simple S-CO_2 Brayton cycle

which helps to avoid common pinch point problems. The fraction of the flow that enters the cooler and the main compressor is an important parameter which directly affects the cycle performance.

Partial Cooling Cycle. This configuration is similar to the recompression cycle, however, one more compressor and cooler are included (Fig. 3). The low pressure flow leaving the LTR cools down in a cooler before entering the precompressor, where the pressure increases to an intermediate value. Then, the flow is divided into two streams: one entering the main compressor after rejecting heat and the other going through the recompression compressor. The two streams are mixed before entering the HTR and receiving heat. In this kind of cycle, the compression is done in two stages and temperature of the working fluid at the inlet of the compressors is lower than the recompression configuration. Kulhánek and Dostal [16] analyzed this cycle and concluded that its efficiency is higher than the recompression configuration at high turbine inlet temperatures. It is also more robust to the variation of the cycle pressure ratio. The pressure ratio of this cycle is usually more than the recompression cycle, which makes it suitable for reheating [11].

Modeling Approach

In order to be consistent with the results presented by Turchi et al. [11], same modeling approach is considered. The following assumptions are made for this study:

(1) Pressure losses in the pipes and heat exchangers are negligible.
(2) Heat loss to the ambient is negligible.
(3) Expansion and compression processes are adiabatic.

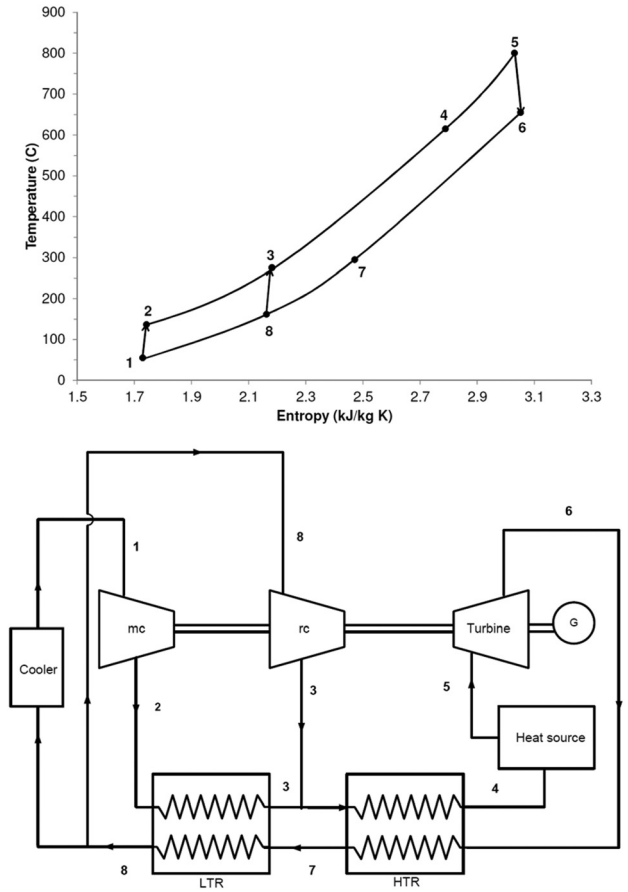

Fig. 2 Recompression S-CO_2 Brayton cycle

(4) Working fluid always achieves the specified temperature at the outlet of the cooler and the heater.
(5) All processes attain steady state.

The recuperators are modeled by defining an effectiveness factor. In the recompression and partial cooling cycles, an effectiveness factor is also considered for the total hot stream [11] which is given as follows:

$$\varepsilon_{\text{hot stream}} = \frac{h_6 - h_8}{h_6 - h_8(T_2, P_8)} \tag{1}$$

In the denominator, the enthalpy at state 8 is calculated based on the assumption that the temperature of the hot fluid leaving LTR reaches the temperature of state 2. Having the enthalpy of the fluid at state 8 using the above formula, the effectiveness of the LTR can be found accordingly. The temperature profiles of the hot and cold streams are obtained by discretizing the heat exchangers along the flow to make sure the minimum temperature difference between the two streams (pinch point) is more than a predetermined value. The output conditions of the compressors and turbines are simply determined by considering a constant isentropic efficiency. The mass fraction of the fluid that goes to LTR in recompression and partial cooling configurations can be found using iteration technique until the temperatures at the outlet of the LTR and recompression compressor (state 3) become almost equal. REFPROP [17] is used to find the properties of CO_2 at different pressures and temperatures.

In order to validate the model, the results can be compared with the available data in the literature. For a minimum cycle temperature of 32 °C, turbine inlet temperature of 550 °C, maximum pressure of 25 MPa, heat exchanger effectiveness of 95%, isentropic compressor efficiency of 89%, and isentropic turbine efficiency of 93%, the maximum cycle efficiency for the simple S-CO_2 Brayton cycle is found as 40.44%. The pressure ratio is obtained as 3.4 by parametric optimization and setting 5 °C as the minimum temperature difference between the hot and cold streams in the recuperator. The efficiencies given by Kulhánek and Dostal [16] and Turchi et al. [11] at the same operating conditions are 40.40% and 40.43%, respectively. The maximum cycle efficiencies at different turbine inlet temperatures for the three configurations are shown and compared with those given by Turchi et al. [11] in Fig. 4.

The cycle pressure ratio for the simple and the recompression cycles is found by parametric optimization. The partial cooling configuration has two design variables, which need to be optimally defined, i.e., the cycle pressure ratio (P_5/P_6) and the intermediate pressure ratio (P_5/P_{10}). A MATLAB [18] code is developed based on genetic algorithms to handle all the required optimization tasks in this study [19].

As can be seen from Fig. 4, the model can accurately predict the efficiency values given by Turchi et al. [11]. It is noteworthy that the turbine efficiency of the recompression cycle was 90% while in other cycles 93% turbine efficiency was used. These are the values used by Turchi et al. [11] for modeling the cycles. The

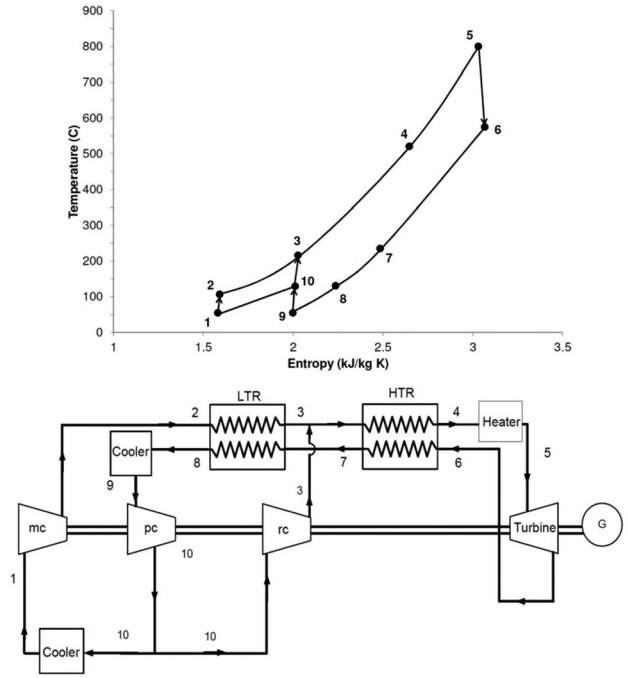

Fig. 3 Partial cooling S-CO_2 Brayton cycle

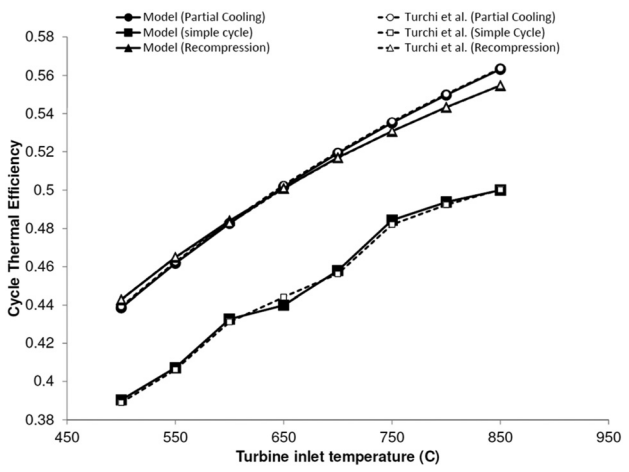

Fig. 4 Validating the model by comparing with the data from Turchi et al. [11]

larger difference between the partial cooling and recompression cycles at high turbine inlet temperatures is due to this assumption.

Combined S-CO_2–ORC Cycle. In this section, an ORC is included with each configuration as a bottoming cycle to utilize the waste heat from the S-CO_2 cycle and generate power. The ORC uses organic working fluids with low boiling points to recover heat from low temperature heat sources. The performance of the ORC is substantially affected by the selection of the working fluid.

The organic working fluids are generally divided into three categories depending on the slope of the saturation curve in the T-s diagram, i.e., wet (e.g., water with negative slope), isentropic (e.g., R11 with vertical slope), and dry (e.g., isopentane with positive slope). The wet fluids usually need to be superheated in order to avoid liquid droplets impingent in the turbine blades during the expansion [20]. In this study, only dry fluids are considered for the ORC cycle, and in all cases, the working fluid enters the turbine in saturated vapor state. Environmental impact of using the organic fluids also needs to be taken into consideration. The main concerns are the ozone depletion potential, global warming potential, and the atmospheric lifetime. Considering these parameters, some working fluids have already been phased out, such as R-11 and R-115, and others, such as R141b and R142b, are planned to be phased out soon. These working fluids are not considered in this study. Although many of the working fluids considered are flammable, this is not a problem as long as proper precautions are taken. Moreover, auto ignition is not a concern in this study, as the maximum operating temperatures of the working fluids are relatively low.

Table 1 provides a list of the working fluids considered in this paper along with their critical properties and a parameter, T_{tmax}, which is the maximum operating temperature limit for each. The reason this value is determined is that at temperatures close to the critical point, the fluid is unstable; therefore, there should be a reasonable distance between the high temperature limit of the cycle and the critical temperature. However, there is not a single interpretation of the reasonable distance in the literature. In this paper, the method proposed by Rayegan and Tao [21] is used. In this method, the highest temperature of the cycle is first limited to a

Table 1 Properties of the working fluids used in this study

Working fluid	T_c (°C)	P_c (MPa)	T_{tmax} (°C)
R-123	183.68	3.66	166.05
R-124	122.28	3.62	102.78
R-227ea	102.8	3	91.09
R-236ea	139.29	3.5	132.69
R-245ca	174.42	3.93	158.13
R-245fa	154.05	3.64	139.38
R-C318	115.23	2.78	106.54
R-365mfc	186.85	3.266	177.21
Benzene	288.87	4.906	273.35
Butane	151.98	3.8	137.36
Butene	146.14	4.005	126.01
C4F10	113.18	2.32	107.14
C5F12	147.41	2.05	144.21
Cis-butene	162.6	4.225	140.46
Cyclohexane	280.45	4.075	274.50
Decane	344.55	2.103	340.10
Heptane	266.98	2.736	261.56
Isobutane	134.66	3.63	120.32
Isobutene	144.94	4.009	126.05
Isohexane	224.55	3.04	216.88
Isopentane	187.25	3.37	177.87
Neopentane	160.59	3.196	152.27
Nonane	321.4	2.281	316.43
Octane	296.17	2.497	290.50
Pentane	196.55	3.37	186.82
Toluene	318.6	4.13	307.46

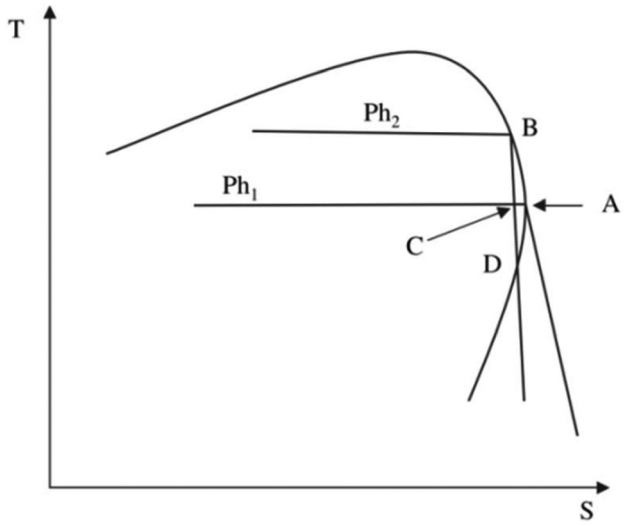

Fig. 5 High temperature limit of the ORC cycle [21]

point on saturation curve where the slope of the T-s diagram is infinity (point A in Fig. 5). Then, this temperature is increased up to a point (B) where further increasing the temperature causes the quality of the working fluid to drop to less than 99% during the expansion process. In Fig. 5, the maximum mass fraction of the liquid is at point C, which is assumed to be less than 1%. It is noteworthy that assuming 99% dryness is more than necessary and the cycle can still operate with lower values without any problem. However, decreasing this value to 90% does not affect the efficiency very much; therefore, the 99% dryness constraint is applied to calculate T_{tmax} in Table 1. REFPROP [17] is used to find the properties of the organic fluids throughout the paper. The input parameters to the model of the combined cycle are given in Table 2. It is assumed that the combined cycle operates in a solar power tower (SPT) plant. SPT technology is deemed advantageous over other CSP technologies due to its ability to achieve high operating temperatures, resulting in greater thermodynamic performance of the power cycle. The maximum temperature of the S-CO_2 cycle in this study is fixed at 800 °C, which is achievable in SPT plants, though higher temperatures can be reached depending on the design of the receiver. The main challenge in the receiver design for the S-CO_2 cycle is the high operating pressure. The maximum pressure of the CO_2 cycle is set at 25 MPa, considering piping availability and flange seal needs [11].

CSP plants are usually located in the areas where water resources are limited; therefore, dry cooling may be preferred over wet cooling. Although dry cooling is less efficient (as the dry bulb temperature is more that the wet bulb temperature) and more expensive than wet cooling, it is an appropriate option for arid areas. A dry bulb temperature of 41 °C represents the 99.8th percentile of the annual temperature distribution in Daggett, CA, therefore,

Table 2 Input parameters to the combined S-CO_2-ORC cycle model

Maximum pressure	25 MPa
Maximum temperature of CO_2 cycle	800 °C
Minimum temperature of ORC and CO_2 cycles	55 °C
Mass flow rate of the S-CO_2 cycle	1 kg/s
Heat exchanger effectiveness	0.95
Total hot stream effectiveness	0.95
Pinch point (minimum temperature difference)	5 °C
CO_2 turbine efficiency	0.90
Compressor efficiency	0.89
ORC turbine efficiency	0.87
ORC pump efficiency	0.85

the minimum temperature of both CO_2 and ORC cycles is set to 55 °C [11].

In the modeling of the recuperators in recompression and partial cooling cycles, the effectiveness of the HTR and the total hot stream are set at 0.95, and the effectiveness of the LTR is found accordingly. The temperature profiles of the hot and cold streams in all the heat exchangers are checked to make sure the pinch point constraint is not violated.

It is important to mention that the range of the pressure ratio considered for the combined cycles during optimization is larger than the stand-alone cycles. In other words, the S-CO_2 turbine is allowed to expand to subcritical pressure with supercritical temperature for all the configurations, yielding transcritical carbon dioxide cycles [14]. The maximum pressure ratio for the simple and recompression configurations is limited to five, while it is extended to seven for the partial cooling cycle.

Combined Simple S-CO_2–ORC Cycle. The combined cycle configuration is shown in Fig. 6. The S-CO_2 goes through the heat recovery unit and provides heat for the ORC cycle before entering the cooler. The maximum mass flow rate of the ORC is found by setting the minimum temperature difference between the hot and cold streams in the heat recovery unit at 5 °C. The S-CO_2 cycle pressure ratio (r_p) and the turbine inlet temperature of the ORC cycle (T_{3R}) are the parameters that need to be optimally determined by maximizing the combined cycle efficiency. This is done for every working fluid listed in Table 1.

Different parameters can be used as the decision criteria for the selection of the working fluids, from which combined cycle efficiency ($\eta_{combined}$) and expansion ratio of the ORC turbine (ϕ) are considered in this study which are defined as follows:

$$\eta_{combined} = \frac{W_{net,CO_2} + W_{net,ORC}}{Q_{in}} \tag{2}$$

$$\phi = \frac{\dot{V}_{4R}}{\dot{V}_{3R}} \tag{3}$$

where $\dot{V}$ represents the volumetric flow rate (m^3/s). For the design of the ORC turbine, the organic fluids with high expansion ratios are not recommended because of supersonic flow problems, larger turbine size or greater number of stages [21]. Figure 7 compares the performance of the combined cycle for different organic fluids. As can be seen, the maximum efficiency is obtained by using isopentane as the ORC fluid, i.e., 0.5216. On the other hand, the

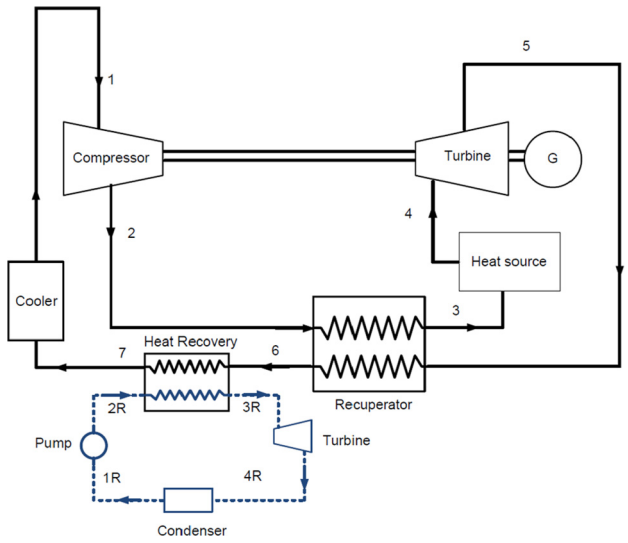

Fig. 6 Combined simple S-CO_2–ORC cycle. The ORC cycle is shown with dashed lines.

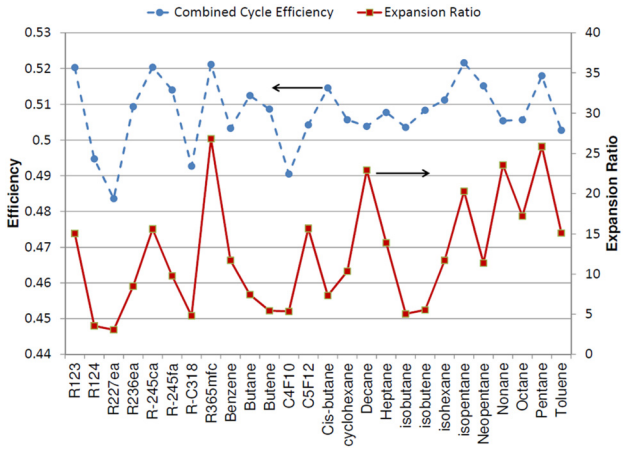

Fig. 7 Performance evaluation of the combined simple S-CO_2-ORC cycle using different organic fluids

Table 3 Operating conditions of the selected working fluids for combined simple S-CO_2-ORC cycle

Working fluid	r_p	T_{3R} °C	P_{max} (MPa)	m_{ORC} $\left(\frac{kg}{s}\right)$	$\eta_{combined}$	ϕ
Butene	4.22	126.01	2.85	0.448	0.5086	5.43
Cis-butene	4.52	140.46	2.96	0.395	0.5146	7.32

ORC turbine expansion ratio for this fluid is very high, i.e., 20.29, which makes it unsuitable for the design of the turbine. The same problem exists for some other working fluids, where the high efficiency is accompanied by a high expansion ratio. The lowest expansion ratio, 3.53, is obtained by R227ea and has a thermal efficiency of 0.4835. Considering both thermal efficiency and expansion ratio as the decision criteria, R236ea, R245fa, butane, butene, cis-butene, and isobutene are shortlisted for further consideration. A comparative analysis of these candidates is used for final selection, e.g., while R245fa has a combined thermal efficiency of 0.5140 and expansion ratio of 9.78, it is less advantageous in comparison with cis-butene with a thermal efficiency of 0.5146 and expansion ratio of 7.32. Finally, butene and cis-butene are selected as the only working fluids that cannot be outperformed by others. Table 3 summarizes the optimal operating conditions for these working fluids. As might be expected, the turbine inlet temperature of the ORC cycle for both fluids is equal to their maximum operating temperature limit, T_{tmax}, that is given in Table 1. Maximum pressure of the ORC cycle (P_{max}) for each working fluid is also given in the table. Higher pressures require thicker pipes and more expensive heat exchangers. The efficiency of the simple S-CO_2 configuration without the bottoming cycle under same operating condition is obtained as 0.4507.

Combined Recompression S-CO_2–ORC Cycle. The combined cycle configuration for the recompression cycle is shown in Fig. 8. As can be seen, a heat recovery unit is included before the cooler and the main compressor. Therefore, only a fraction of the total mass flow rate of S-CO_2 enters the heat recovery unit. Including the heat recovery before splitting the mass and right after the LTR reduces the temperature of the flow entering the recompression compressor. Consequently, the temperature at point 3 decreases which negatively affects the performance of the cycle.

Similar to the combined simple S-CO_2-ORC cycle, the recompression S-CO_2 cycle pressure ratio and the turbine inlet temperature of the ORC cycle are determined by maximizing the combined cycle efficiency.

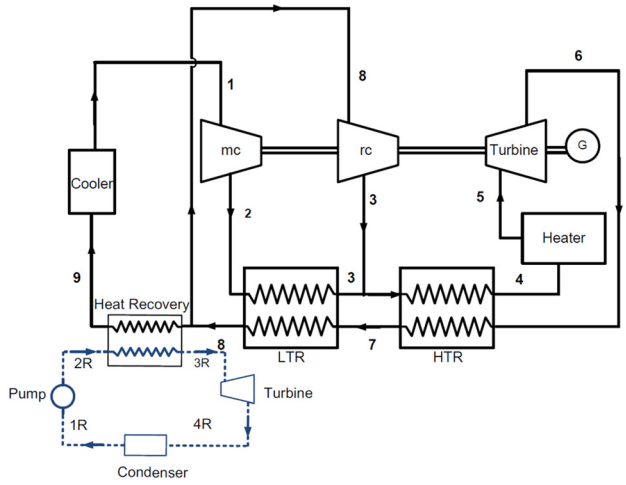

Fig. 8 Combined recompression S-CO_2-ORC cycle

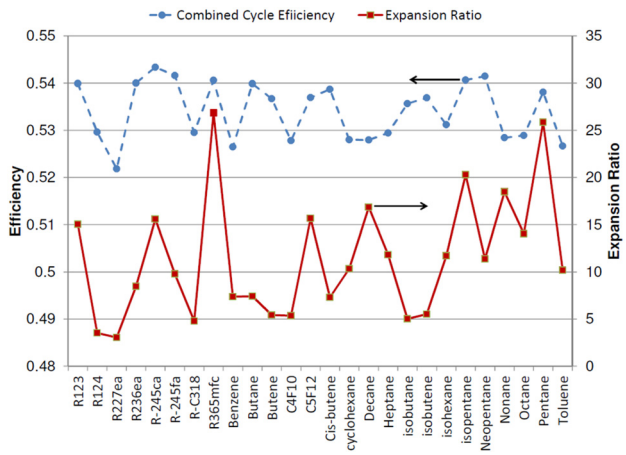

Fig. 9 Performance evaluation of the combined recompression S-CO_2-ORC cycle using different organic fluids

The performance of the combined cycle under optimal condition for each working fluid is shown in Fig. 9. The maximum efficiency is obtained by using R245ca, i.e., 0.5433, with an impractical expansion ratio of 15.61. The minimum expansion ratio is obtained by using R227ea, i.e., 3.05, where the maximized thermal efficiency is equal to 0.5218. Following the same procedure as explained in the S-CO_2 Brayton Cycle Configurations section, six working fluids are found as superior to the others, which are given in Table 4. The turbine inlet temperature of the ORC cycle for all the fluids is equal to their maximum operating temperature limit, T_{tmax}, which is given in Table 1. The efficiency of the recompression S-CO_2 configuration without the bottoming cycle under same operating condition is obtained as 0.4932.

Table 4 Operating conditions of the selected working fluids for combined recompression S-CO_2-ORC cycle

Working fluid	r_p	T_{3R} °C	P_{max} (MPa)	$m_{ORC}\left(\frac{kg}{s}\right)$	$\eta_{combined}$	ϕ
R236ea	3.45	132.69	2.99	0.671	0.5400	8.48
R245fa	3.84	139.38	2.79	0.58	0.5416	9.78
Butane	3.84	137.36	2.98	0.299	0.5398	7.43
Butene	3.45	126.01	2.85	0.285	0.5367	5.42
Cis-butene	4.13	140.46	2.96	0.286	0.5387	7.32
Isobutane	3.26	120.32	2.85	0.280	0.5357	5.03

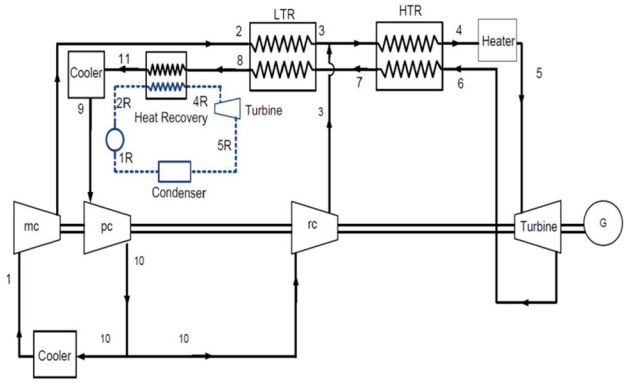

Fig. 10 Combined partial cooling S-CO_2-ORC cycle

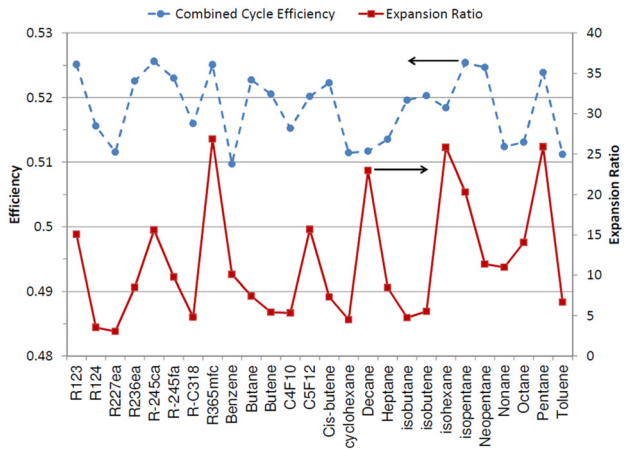

Fig. 11 Performance evaluation of the combined partial cooling S-CO_2-ORC cycle using different organic fluids

Table 5 Operating conditions of the selected working fluids for combined Partial cooling S-CO_2-ORC cycle

Working fluid	r_p	r_{pp}	T_{3R} °C	P_{max} (MPa)	$m_{ORC}\left(\frac{kg}{s}\right)$	$\eta_{combined}$	ϕ
R124	5.39	2.95	102.78	2.51	0.81	0.5156	3.53
R245fa	6.52	4.08	139.38	2.79	0.71	0.5230	9.78
Butane	5.71	3.92	137.36	2.98	0.36	0.5228	7.43
Butene	5.87	3.59	126.01	2.86	0.35	0.5205	5.42
Cis-butene	6.19	4.24	140.46	2.96	0.35	0.5223	7.32
Isobutane	5.39	3.11	120.32	2.85	0.34	0.5196	4.76

Combined Partial Cooling S-CO_2–ORC Cycle. The combined cycle layout is shown in Fig. 10. After leaving the LTR, the low pressure S-CO_2 enters the heat recovery unit and provides heat for the bottoming cycle. There are three parameters that need to be optimally determined by maximizing the combined cycle efficiency, i.e., cycle pressure ratio $(r_p = P_5/P_6)$, intermediate pressure ratio $(r_{pp} = P_5/P_{10})$, and the ORC turbine inlet temperature (T_{3R}). The maximized thermal efficiency and the corresponding turbine expansion ratio of the combined cycle for each working fluid are shown in Fig. 11. Similar to the recompression cycle, the maximum efficiency is obtained by using R245ca, i.e., 0.5256, with an expansion ratio of 15.61. The minimum expansion ratio, which is 3.05, is also obtained for R227ea with a maximized thermal efficiency of 0.5115. The final recommended list of the working fluids for the combined partial cooling S-CO_2–ORC cycle is given in Table 5. The maximum operating pressures for

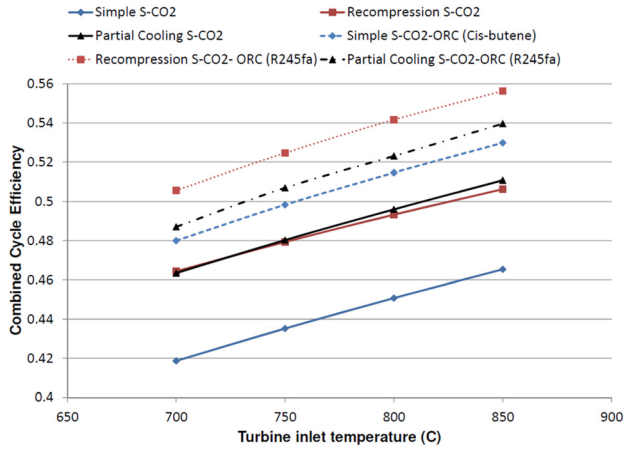

Fig. 12 Performance comparison of the combined and the single cycles at different turbine inlet temperatures

all the working fluids, except R124, are similar to those given in Table 4. The maximum pressure of R124 is 2.51 MPa. The efficiency of the partial cooling S-CO_2 configuration without the bottoming cycle under same operating condition is obtained as 0.4959.

Discussion and Conclusion

According to the results presented in Modeling Approach sections, adding an appropriate bottoming cycle can increase the overall cycle efficiency by 3–7% points under the specified conditions. The largest efficiency increase is achieved by using a simple S-CO_2 as the top cycle. However, this cycle is less efficient than the recompression and the partial cooling cycles. The maximum combined cycle efficiency is obtained by the recompression S-CO_2-ORC cycle.

In order to make sure this conclusion is valid at other heat source temperatures also, the turbine inlet temperature is varied from 700 °C to 850 °C. Performances of the S-CO_2 cycles (without bottoming cycles) and the combined cycles are optimized at each temperature. The organic working fluid used for each configuration is the one with maximum efficiency, which is given in the recommended lists (Tables 3–5), i.e., cis-butene for the simple cycle, R245fa for the recompression and the partial cooling cycles. The results are presented in Fig. 12.

The efficiencies of the partial cooling and the recompression cycles are almost equal at similar temperatures, however, the recompression cycle presents a higher overall potential when used as the top cycle in conjunction with an ORC. In addition, the recompression cycle operates at lower pressure ratios that can be considered as an advantage over the partial cooling cycle.

Among the working fluids considered for the ORC, butene and cis-butene are found to be most appropriate for each of the combined cycle configurations on the basis of global efficiency and expansion ratio. Final selection of the working fluid, however, would necessarily include consideration of these factors and other relevant criteria that are outside the scope of this study, e.g., availability and cost of suitable turbomachinery, compromise between heat exchanger pressure rating and cost, operational issues (freezing point, negative condenser pressure, pump cavitation) fluid toxicity, and tribological factors, etc.

Nomenclature

Abbreviations

HTR = high temperature recuperator
LTR = low temperature recuperator
mc = main compressor
pc = precompressor
rc = recompression compressor

Greek Symbols

h = enthalpy (kJ/kg)
m_{ORC} = mass flow rate of ORC (kg/s)
P = pressure (MPa)
P_c = critical pressure (MPa)
P_{max} = maximum operating pressure of the ORC (MPa)
Q_{in} = input heat to the top cycle (kJ/kg)
r_p = cycle pressure ratio
r_{pp} = intermediate pressure ratio
T = temperature (°C)
T_c = critical temperature (°C)
T_{tmax} = temperature limit of the organic fluid (°C)
T_{3R} = maximum operating temperature of the ORC (°C)
V = volumetric flow rate (m^3/s)
W_{net} = net power generated (kJ/kg)
ε = heat exchanger effectiveness
$\eta_{combined}$ = thermal efficiency of the combined cycle
ϕ = ORC turbine expansion ratio

References

[1] Feher, E. G., 1967, "Supercritical Thermodynamic Power Cycle," Proceeding of the IECEC, Miami Beach, FL, August 13–17.
[2] Angelino, G., 1967, "Perspectives for the Liquid Phase Compression Gas Turbine," ASME J. Eng. Power, **89**, pp. 229–237.
[3] Angelino, G., 1968, "Carbon Dioxide Condensation Cycles for Power Production," ASME J. Eng. Power, **90**, pp. 287–295.
[4] Angelino, G., 1969, "Real Gas Effects in Carbon Dioxide Cycles," ASME Paper No. 69-GT-103.
[5] Dostal, V., Hejzlar, P., and Driscoll, M. J., 2006, "The Supercritical Carbon Dioxide Power Cycle: Comparison to Other Advanced Power Cycles," Nucl. Technol., **154**(3), pp. 283–301.
[6] Sarkar, J., 2009, "Second Law Analysis of Supercritical CO_2 Recompression Brayton Cycle," Energy, **34**(9), pp. 1172–1178.
[7] Sarkar, J., and Bhattacharyya, S., 2009, "Optimization of Recompression S-CO_2 Power Cycle With Reheating," Energy Convers. Manage., **50**(8), pp. 1939–1945.
[8] Moisseytsev, A., and Sienicki, J. J., 2009, "Investigation of Alternative Layouts for the Supercritical Carbon Dioxide Brayton Cycle for a Sodium-Cooled Fast Reactor," Nucl. Eng. Des., **239**(7), pp. 1362–1371.
[9] Jeong, W. S., Lee, J. I., and Jeong, Y. H., 2011, "Potential Improvements of Supercritical Recompression CO_2 Brayton Cycle by Mixing Other Gases for Power Conversion System of a SFR," Nucl. Eng. Des., **241**(6), pp. 2128–2137.
[10] Turchi, C. S., 2009, "Supercritical CO_2 for Application in Concentrating Solar Power Systems," Proceedings of SCCO2 Power Cycle Symposium, Troy, NY, April 29–30.
[11] Turchi, C. S., Ma, Z., Neises, T., and Wagner, M., 2012, "Thermodynamic Study of Advanced Supercritical Carbon Dioxide Power Cycles for High Performance Concentrating Solar Power Systems," ASME 2012 6th International Conference on Energy Sustainability (ES2012), San Diego, CA, July 23–26, ASME Paper No. ES2012-91179.
[12] "SunShot Initiative," 2013, U.S. Department of Energy, www1.eere.energy.gov/solar/sunshot/
[13] Hung, T. C., Shai, T. Y., Wang, S. K., 1997, "A Review of Organic Rankie Cycles (ORCs) for the Recovery of Low-Grade Waste Heat," Energy, **22**(7), pp. 661–667.
[14] Chacartegui, R., Muñoz de Escalona, J. M., Sánchez, D., Monje, B., and Sánchez, T., 2011, "Alternative Cycles Based on Carbon Dioxide for Central Receiver Solar Power Plants," Appl. Therm. Eng., **31**(5), pp. 872–879.
[15] Sánchez, D., Brenes, B. M., de Escalona, J. M. M., and Chacartegui, R., 2012, "Non-Conventional Combined Cycle for Intermediate Temperature Systems," Int. J. Energy Res., **37**(5), pp. 403–411.
[16] Kulhánek, M., and Dostal, V., 2011, "Supercritical Carbon Dioxide Cycles Thermodynamic Analysis and Comparison," Supercritical CO_2 Power Cycle Symposium, Boulder, CO, May 24–25.
[17] Lemmon, E. W., McLinden, M. O., and Huber, M. L., "NIST Reference Fluid Thermodynamic and Transport Properties—REFPROP," National Institute of Standards and Technology, Gaithersburg, MD, NIST Standard Reference Database 23.
[18] McDonald, C. F., 2003, "Recuperator Considerations for Future Higher Efficiency Microturbines," Appl. Therm. Eng., **23**(12), pp. 1463–1487.
[19] Demirkaya, G., Besarati, S., Vasquez Padilla, R., Ramos Archibold, A., Goswami, D. Y., Rahman, M. M., and Stefanakos, E. L., 2012, "Multi-Objective Optimization of a Combined Power and Cooling Cycle for Low-Grade and Mid-grade Heat Sources," ASME J. Energy Resour. Technol., **134**(3), p. 032002.
[20] Chen, H., Goswami, D. Y., and Stefanakos, E. K., 2010, "A Review of Thermodynamic Cycles and Working Fluids for the Conversion of Low-Grade Heat," Renewable Sustainable Energy Rev., **14**(9), pp. 3059–3067.
[21] Rayegan, R., and Tao, Y. X., 2011, "A Procedure to Select Working Fluids for Solar Organic Rankine Cycles (ORCs)," Renewable Energy, **36**(2), pp. 659–670.